PATTERN DESIGN FOR NON-GEODESIC WINDING TOROIDAL PRESSURE VESSELS

Lei Zu*, Qin-Xiang He*, Qing-Qing Ni**
** Dept. of Engineering Mechanics, Xi'an University of Technology, Xi'an 710054, China,*
*** Dept. of Functional Machinery and Mechanics, Shinshu University, Ueda 386-8576, Japan*

Keywords: *Filament winding; Toroidal pressure vessels; Pattern design; Non-geodesic pattern; Structural optimization; CAD*

Abstract

A design-oriented method for non-geodesic winding toroidal pressure vessels was described systematically in this paper. The differential equations of non-geodesic on torus were derived from differential geometry. Structural optimization procedure for non-geodesic pattern was presented. The transmission relationship between the toroidal mandrel and the payout eye was given. The optimum pattern was adjusted based on conditions of uniform and full coverage. The movement equations of winding machine for torus were obtained. The main frame of CAD system was investigated and simulations of non-geodesic trajectories were performed. The results show that the winding angle of optimum non-geodesic is about 10 to 15 degree smaller than that of geodesic. The structural performance of toroidal vessel is remarkably promoted by utilizing this pattern. The key modules of CAD system are realized and the optimum pattern satisfies winding principles. It can be regarded as the theoretical foundation of computer aided filament winding toroidal vessels.

1 Introduction

Filament winding composite materials are widely used in multi-industrial fields where weight reduction of the infrastructure is required because of its high specific modulus and specific strength. Pressure vessels using this composite material in comparison with conventional metal vessels can be applied in fields such as the defence industry, aerospace industry and rocket motor casings where light weight but resistance to high pressure is demanded. In recent years, there are a number of publications on axisymmetric filament winding on convexity [1-4], including composite cylinder, sphere and cone. However, there have been few investigations with respect to filament winding toroidal pressure vessels, and just limit to the geodesic winding pattern [5,6]. When winding an axisymmetric part, a basic fiber path is repeated continuously by indexing the winding axis, opposed to torus, which is non-axisymmetric body and has a concave. On the other hand, due to the high load applied to it, the process of filament winding toroidal pressure vessels is different from that of winding elbows in civilian use. It is well-known that the geodesic is the most stable on a curved surface, and the computation of fiber path is relatively easy with only a Clariaut equation. But the geodesic pattern is completely dependent on the initial winding conditions, and the angle of the stable geodesic is rather big in general [7]. So the geodesic cannot take full advantage of the mechanics performance of filaments. Moreover, the winding parameters of geodesic pattern cannot be optimized for enhancing structural characteristics such as strength, stiffness, *etc*. Authors' research group put forward the equicohesive pattern [8] and its optimization method [9] to enhance the structural strength. Although toroidal vessels wound by the equicohesive pattern possess great strength, it is difficult to realize the strict steady-conditions. Therefore, it is necessary for filament winding toroidal pressure vessels to adopt non-geodesic winding method, in order to meet structural optimization and winding stability at the same time.

This paper researches into method to design fiber paths of filament winding toroidal pressure vessels, generalizes non-geodesic pattern and structural optimization method in the traditional winding, successfully applies them to the fiber path

design of winding toroidal vessels, presents mathematical principles and movement equations of winding torus, and develops a computer aided filament winding system for toroidal vessels fabrication.

2 Non-geodesic pattern

A toroidal vessel is a general shell of revolution with circle areas surrounding the rotational axis defined as *Z*-axis. $S(\theta,\varphi)$ is taken to be the vector representation of the torus, which can be expressed as

$$\boldsymbol{S}(\theta,\varphi)=\begin{Bmatrix}(R+r\cos\varphi)\cos\theta\\(R+r\cos\varphi)\sin\theta\\r\sin\varphi\end{Bmatrix}$$

where θ and φ stand for the geometry parameters of the torus, as shown in Fig.1.

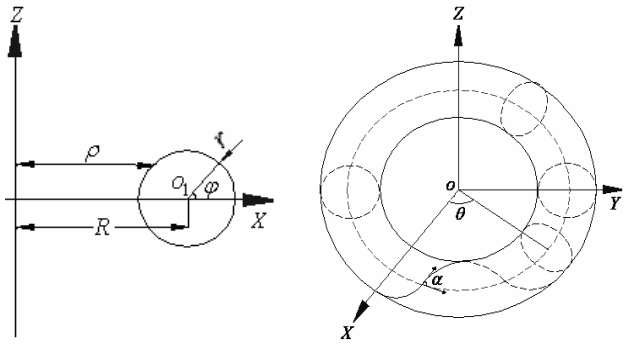

Fig.1. Sign convention for coordinates and the position of the fiber on a toroidal shell

The winding tension induced by the payout eye may drive the fiber to slip on surface and to bridge on concave. The equation for describing the slip trend can be given as

$$\lambda = K_g / K_n \qquad (1)$$

where λ is the slippage resistance; K_g and K_n are the geodesic curvature and the normal curvature, respectively.

The first fundamental form of $S(\theta,\varphi)$ can be obtained by differential geometry:

$$E=(R+r\cos\varphi)^2,\ F=0,\ G=r^2 \qquad (2)$$

Substituting Eq. (2) into Liouville formula, K_g can be easily calculated:

$$K_g=\frac{d\alpha}{ds}+\frac{\sin\varphi}{R+r\cos\varphi}\cos\alpha \qquad (3)$$

where α is the acute angle between the tangent to fiber path and the parallel direction of the torus, i.e. winding angle; s is the length of the fiber curve.

K_n can be expressed in terms of a couple of curvatures as Euler formula form:

$$K_n=K_\theta\cos^2\alpha+K_\varphi\sin^2\alpha$$

where K_θ and K_φ are the curvature of meridian and the curvature of parallel on torus, respectively.

From differential geometry, we have:

$$k_\theta=-\frac{\cos\varphi}{R+r\cos\varphi},\ k_\varphi=-\frac{1}{r},$$

namely

$$K_n=-\frac{\cos\varphi}{R+r\cos\varphi}\cos^2\alpha-\frac{1}{r}\sin^2\alpha \qquad (4)$$

Substituting Eqs. (3) and (4) into Eq. (1), we get the differential equation of the non-geodesic on torus, given by

$$\frac{d\alpha}{ds}=-\left(\frac{\cos\varphi}{R+r\cos\varphi}\cos^2\alpha+\frac{1}{r}\sin^2\alpha\right)\lambda-\frac{\sin\varphi}{R+r\cos\varphi}\cos\alpha \qquad (5)$$

The relationship between geometrical parameters of the torus can be shown as:

$$\frac{d\theta}{ds}=\frac{\cos\alpha}{R+r\cos\varphi},\quad \frac{d\varphi}{ds}=\frac{\sin\alpha}{r} \qquad (6)$$

Substituting Eq. (6) into Eq. (5), after some transformations, Eq. (5) is reduced to the steady equations of non-geodesic winding on torus as follows:

$$\begin{cases}\dfrac{d\alpha}{d\varphi}=-\left[\dfrac{r\cos\varphi\cos\alpha}{(R+r\cos\varphi)tg\alpha}+\sin\alpha\right]\lambda-\dfrac{r\sin\varphi}{(R+r\cos\varphi)tg\alpha}\\[2ex]\dfrac{d\alpha}{d\theta}=-\left[\cos\varphi\cos\alpha+\dfrac{(R+r\cos\varphi)tg\alpha\sin\alpha}{r}\right]\lambda-\sin\varphi\end{cases} \qquad (7)$$

Obviously, let $\lambda=0$, the well-known Clariaut equation can be deduced by Eqs. (7):

$$(R+r\cos\varphi)\cos\alpha=C$$

where C is a constant value determined by initial wind angle α_0.

If $\lambda\neq 0$, there are no analytical solutions for the steady equations (7). According to the boundary conditions of winding process, the non-geodesic trajectory can be calculated step by step by *Runge-Kutta* method. Then, several characteristic parameters for pattern design are obtained. From Eqs. (7), we know that the design and adjustment of non-geodesic winding pattern are more controllable than geodesic because of more DOF.

In order to avoid fiber slippage and bridging,

the winding pattern should meet the steady-conditions as follows [10]:

$$|\lambda| \le \mu \text{ and } k_n < 0 \qquad (8)$$

where μ is the friction coefficient between the filament and the wound surface, which should be tested by friction measurement.

From Eqs.(4) and (8), for torus, it is impossible to bridge on convexity as a permanent result of $k_n < 0$. Whereas, the winding angle of the fiber on concave should satisfy the following condition to avoid bridging:

$$\alpha > tg^{-1}\sqrt{\frac{-r\cos\varphi}{R + r\cos\varphi}}$$

From Eqs. (7) and (8), we can get the following condition to avoid fiber slippage:

$$\lambda = \left| \frac{\frac{d\alpha}{d\varphi}\cdot\sin\alpha + \frac{r\sin\varphi}{R + r\cos\varphi}\cos\alpha}{\frac{r\cos\varphi}{R + r\cos\varphi}\cos^2\alpha + s\,\mathrm{in}^2\alpha} \right| \le \mu$$

3 Optimum Structural Design

The structural performance plays an important role in composite pressure vessels of aircraft. A compromise between manufacturing ease and design requirements must be sought. With optimization technique and mechanics of composites, the winding pattern can be optimized to reduce fabrication cost and improve storage mass efficiency of the propellant, the security, maneuverability of the vessels. There are many design demands for winding pressure vessels, including strength, stiffness, non-bridging, non-slippage, uniform and full coverage, dynamic stability, *etc*. The optimization objective can be chosen as weight, burst pressure, structural stiffness, stability, *etc*. According to the fabrication conditions and the actual demands, the appropriate requirements and the main purpose are selected as design constraints and the main purpose as objective function. For instance, the weight is treated as optimization objective while the demand of strength, stiffness, winding stability and burst pressure are treated as constraint condition at the same time. We optimize the initial wind angle, the thickness of different layers and the slippage resistance using SQP algorithm to minimize the weight. Flow chart of optimization program is shown in Fig.2. Structural optimization can be regarded as the theoretical foundation of pattern design.

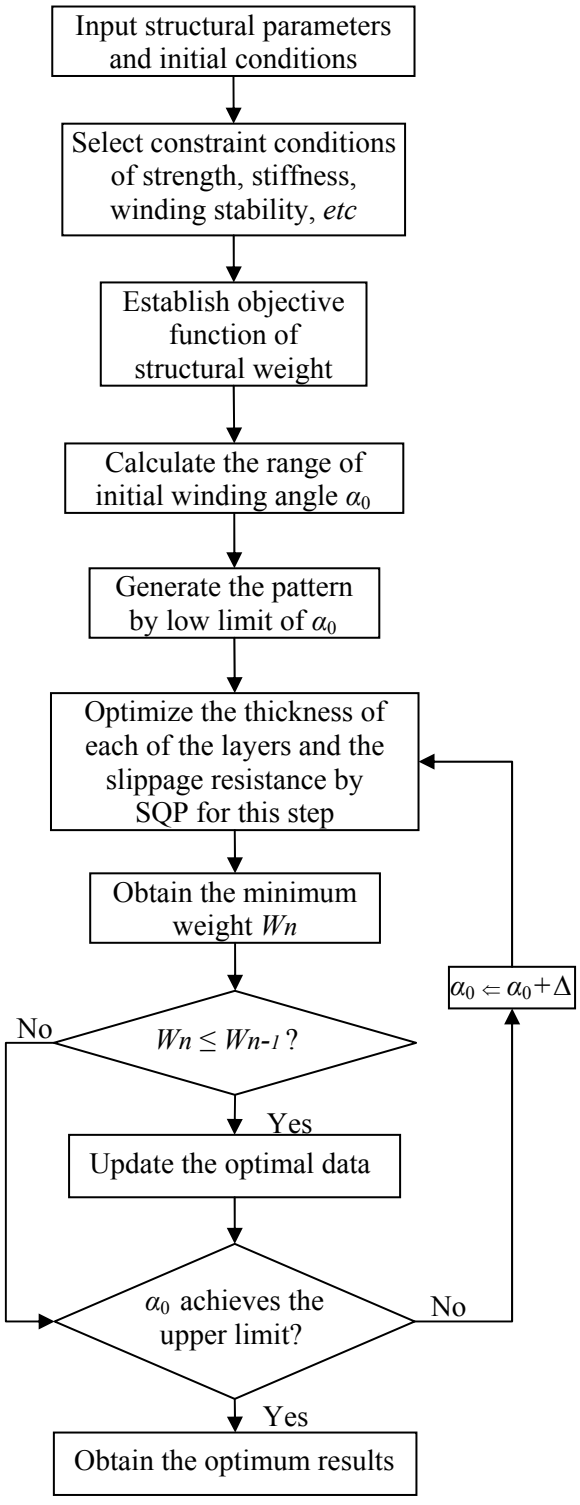

Fig.2 Flow chart of structural optimization

4. Movement Model of the Winding Machine

This research considers here a three-dimensional mandrel model attached to a winding machine. The mathematical model of determining the position of the payout eye is outlined as follows.

The fiber coming from the payout eye is always tangent to the surface of the mandrel, as shown in Fig. 3. The tangent point P is called doffing point along the geodesic curve on the mandrel surface. *o-xyz* fixed to the mandrel is the moving coordinate, where axis z is overlapping with the rotational axis. *O-XYZ* is the static coordinate system and plane *O-XZ* is parallel to eye moving plane. The moving coordinates move around axis Z. Φ is the rotation angle of the moving coordinates relative to static coordinates.

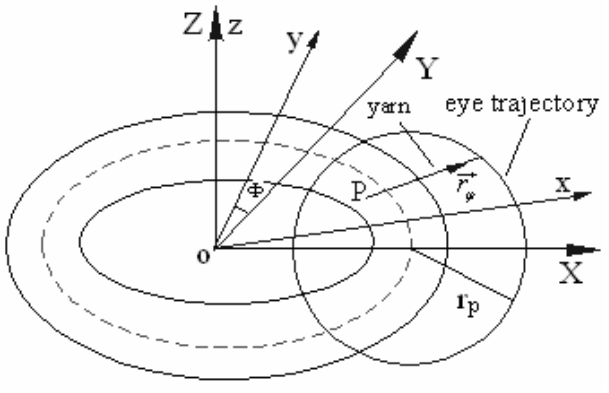

Fig.3. Coordinate system of the winding machine

Assuming that axis *ox* is overlapping with the axis *OX* in the original position, the relationship between the moving coordinates and static coordinates is expressed as follows:

$$\begin{Bmatrix} x \\ y \\ z \end{Bmatrix} = \begin{Bmatrix} \cos\Phi & \sin\Phi & 0 \\ -\sin\Phi & \cos\Phi & 0 \\ 0 & 0 & 1 \end{Bmatrix} \begin{Bmatrix} X \\ Y \\ Z \end{Bmatrix} \tag{9}$$

In terms of the vector representation of the torus, the coordinates of point P can be defined as

$$\vec{P} = \{(R + r\cos\varphi)\cos\theta, (R + r\cos\varphi)\sin\theta, r\sin\varphi\}$$

Then the directional derivative of the non-geodesic curve passing through point P is

$$\vec{r_\varphi} = \begin{Bmatrix} -r\sin\varphi\cos\theta - (R + r\cos\varphi)\sin\theta \cdot \theta'_\varphi \\ -r\sin\varphi\sin\theta + (R + r\cos\varphi)\cos\theta \cdot \theta'_\varphi \\ r\cos\varphi \end{Bmatrix}^{\mathrm{T}}$$

The tangent equations which connect the doffing point P to the putout eye can be written as

$$\begin{aligned} \frac{x-(R+r\cos\varphi)\cos\theta}{\sin\theta-\mathrm{tg}\alpha\sin\varphi\cos\theta} &= \frac{y-(R+r\cos\varphi)\sin\theta}{-\cos\theta-\mathrm{tg}\alpha\sin\varphi\sin\theta} \\ &= \frac{z-r\sin\varphi}{\mathrm{tg}\alpha\cos\varphi} \end{aligned} \tag{10}$$

Substituting Eq. (9) into Eq. (10) becomes

$$\begin{aligned} &\frac{X-(R+r\cos\varphi)\cos(\theta+\Phi)}{\sin(\theta+\Phi)-\mathrm{tg}\alpha\sin\varphi\cos(\theta+\Phi)} \\ &= \frac{Y-(R+r\cos\varphi)\sin(\theta+\Phi)}{-\cos(\theta+\Phi)-\mathrm{tg}\alpha\sin\varphi\sin(\theta+\Phi)} \\ &= \frac{Z-r\sin\varphi}{\mathrm{tg}\alpha\cos\varphi} \end{aligned}$$

Let Y=0, above equations can be rewritten as

$$\begin{cases} X = \dfrac{R+r\cos\varphi}{\cos(\theta+\Phi)+\mathrm{tg}\alpha\sin\varphi\sin(\theta+\Phi)} \\ Z = r\sin\varphi + \dfrac{(R+r\cos\varphi)\mathrm{tg}\alpha\cos\varphi\sin(\theta+\Phi)}{\cos(\theta+\Phi)+\mathrm{tg}\alpha\sin\varphi\sin(\theta+\Phi)} \end{cases} \tag{11}$$

Eq. (11) is the eye movement equations. Additionally, the eye trajectory is a circle with radius r_p. Apparently, the eye coordinates can be also related by

$$X^2 + Z^2 = r_p^{\,2} \tag{12}$$

The nonlinear equation for the mandrel rotation angle can be derived by substituting Eq. (11) into Eq. (12). Accompanied with the non-geodesic Eq. (7), the rotation angle of the mandrel can be solved by *Newton* method with initial conditions, and the eye coordinates are obtained by Eq. (11). In the practical work, the errors of the fiber path may be accumulated owing to the errors of numerical solution for the nonlinear Eq. (12).

5. Conditions of uniform and Full Coverage

Assuming that the payout eye take K turns around Y-axis in the fixed plane *O-XZ* while the toroidal mandrel take N turns around Z-axis, the ratio of winding velocity can be defined as:

$$i = \frac{\omega_m}{\omega_p} = \frac{N}{K}$$

where N and K are relative prime. Considering proportional and full coverage, we need a tiny adjustment as follows:

$$\Delta i = \frac{w}{2\pi K(R+r)\sin\alpha_0}$$

where w denotes the tape width. Thereout we obtain a fitter ratio of winding velocity for full coverage:

$$i = \frac{N}{K} \pm \frac{w}{2\pi K(R+r)\sin\alpha_0}$$

where '±' determine whether the final doffing point exceed or lag the starting point.

Scilicet, the mandrel rotation angle corresponding to each round of the eye can be described as follows:

$$\theta_m = \frac{2\pi}{K}\left[N \pm \frac{w}{(R+r)\sin\alpha_0}\right]$$

The proportional fiber yarns can completely cover the mandrel surface with absence of gaps if the rotation angle of the mandrel meets above equation. Flow chart of winding pattern adjustment can be given by Fig. 4 based on the condition of uniform and full coverage.

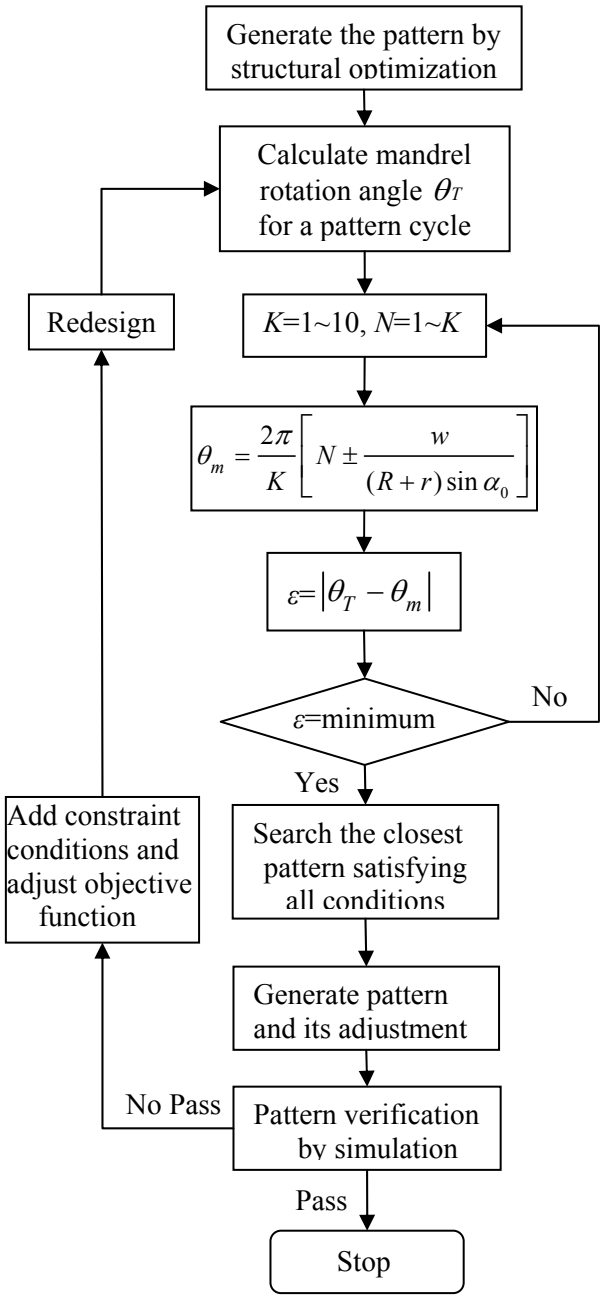

Fig.4. Flow chart of pattern adjustment

6. Configuration of the CAD system

The period design and research will be shortened and operating cost will be reduced by CAD system. The task of computer-human to inputting and outputting parameters interaction is completed well by this system. It is composed of four modules, which are the input and shape treatment, the winding manner selection, the pattern optimization and the winding simulation. A functional description of the modules of the system is presented in brief as follows.

6.1 Input and shape treatment module

The shape treatment is a preliminary step to generate a mandrel model of a composite pressure vessel. It automatically generates the shape of the composite pressure vessel as a three-dimensional shape driven by input data. For the sake of realizing the interaction of graphics, we must parameterize the model and enactment several groups of parameters. The system can adjust the geometrical parameter timely according to the designer's demand.

6.2 Winding mode selection module

Filament-wound products are produced by using one of three basic types of winding patterns: polar, helical, and hoop. The choices made are based on the shape of the part and the reinforcement orientations required. Polar winding is used to lay down fiber close to 0° to the meridian axis. Helical winding is used to lay fiber at angles from 5° to 80° to the meridian axis. These fibers are wound on the mandrel surface in alternating positive and negative orientations and result in a double layer of wound material. Hoop winding is a special form of helical winding and is used to deposit fiber close to 90° to the meridian axis. The system can combine several winding manners such as symmetrical winding, helical with hoop winding, *etc*.

6.3 Pattern optimization module

With the constraint conditions of design requirements and the optimization objective, the winding pattern can be optimized in this module by optimization procedure and appropriate adjustment based on conditions of uniform and full coverage.

6.4 Winding simulation module

We utilize a simulation system to monitor the winding process, and the improvement can be attained after redesigning. Simulation system has many functions such as mapping, prospect, transformation and lighten calculation. The quality of seeming real can realized by using the relational

commands and functions which includes bitmap, texture, material and color just like the virtual object. The simulation of athletics and scene is implemented by prospect transformation, projection transformation, opacity and so on. The simulating *FW* pattern plays an important role in directing the real *FW*. We can correct the winding pattern and redesign the parameters continuously until the pattern satisfies design demands.

7. Numerical examples and simulations

In the following example, a toroidal mandrel taken as a design objective was supplied by Xi'an Aerospace Composite Materials Institute, where R=512mm, r=132mm. The tensile strength of the winding filament is 4.9GPa, while the burst pressure is 70MPa. Based on the pattern optimization, we plot the static movement coordinates of the payout eye at different time from 0s to 35s. See Fig.5. To further indicate the relative position of the eye and the mandrel, X-coordinate corresponding to φ which denotes the position of the doffing point P is shown in Fig.6.

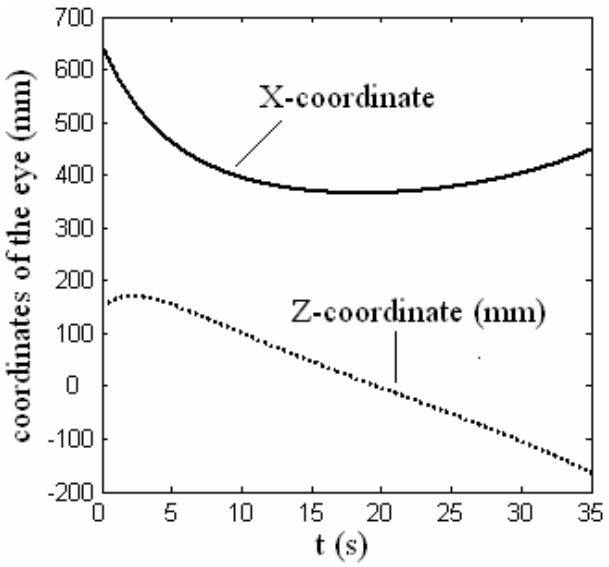

Fig.5. Static coordinates of the eye at different time

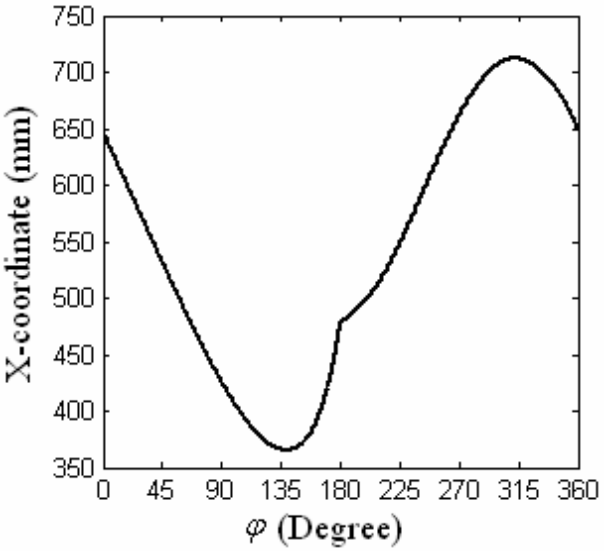

Fig.6 X-coordinate at different φ

In addition, simulation results shown in Figs. 7~10 illustrate the optimum non-geodesic trajectory for single and symmetrically helical winding at different rotations of the mandrel. As shown in simulation results, we can see the winding angle of optimized non-geodesic pattern is about 10 to 15 degree smaller than that of geodesic pattern used in general.

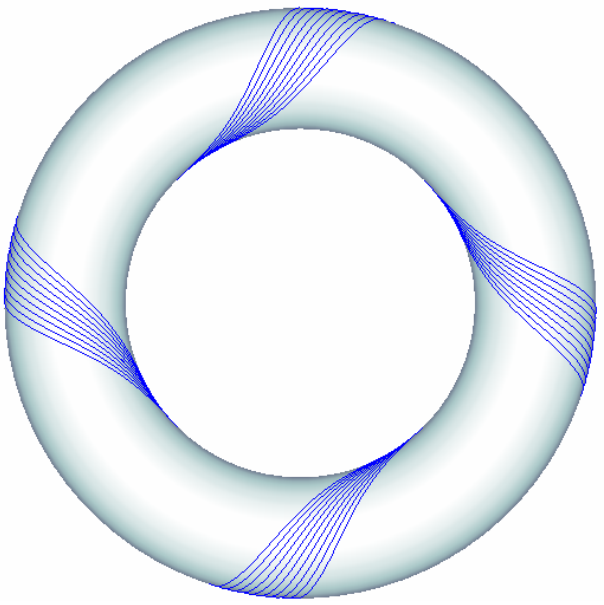

Fig.7. Optimum non-geodesic pattern corresponding to single helical winding at 10 rotations of the mandrel

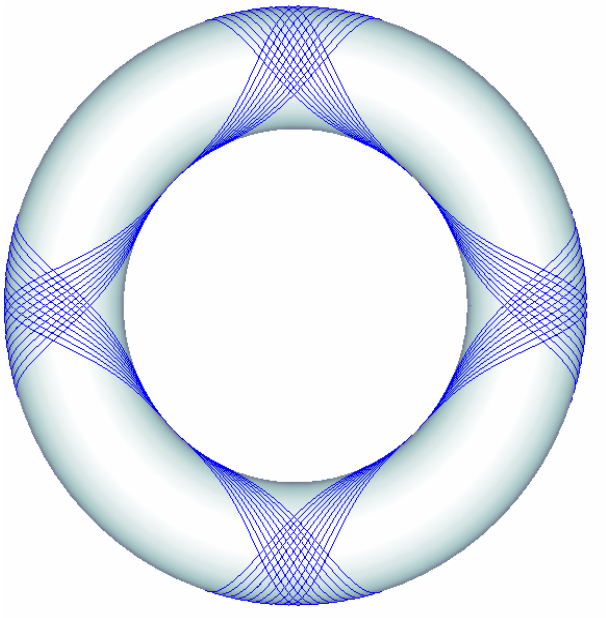

Fig.8. Optimum non-geodesic pattern corresponding to symmetrically helical winding at 10 rotations of the mandrel

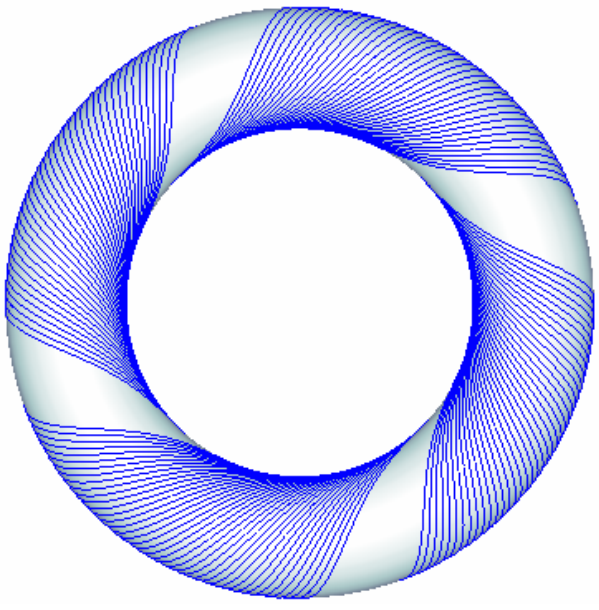

Fig.9. Optimum non-geodesic pattern corresponding to single helical winding at 40 rotations of the mandrel

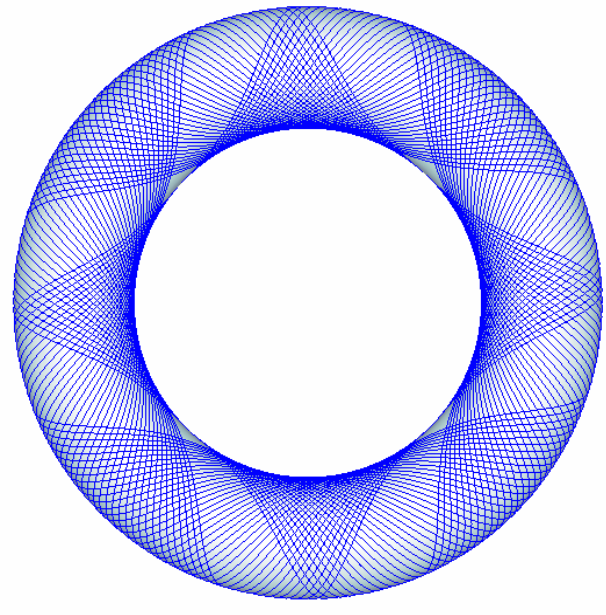

Fig.10. Optimum non-geodesic pattern corresponding to symmetrically helical winding at 40 rotations of the mandrel

8. Conclusion

This study developed a computer aided filament winding system for the manufacturing of composite toroidal pressure vessels using non-geodesic pattern. It considers several factors, such as pattern optimization, the movement mathematics model of the winding machine and computer simulation for verifying the pattern, *etc*. In the light of the outcome of the simulating, we see the winding pattern according with the mathematics equation. Compared to the geodesic pattern, the simulation results can also illustrate the non-geodesic pattern maximize strength of filaments, due to smaller winding angle. Based on the above winding mathematical model, we have succeeded in realizing the combination winding of toroidal pressure vessel. The following Fig.11 shows a finished toroidal pressure vessel wound by non-geodesic pattern. Thereby the soundness and practicality of the mathematical model are verified. The presented patterns and the criteria for stable winding are valuable and practicable in design and manufacture for congener production.

Acknowledgement

The authors would like to thank Xi'an Aerospace Composite Materials Institute for its technical support and sample preparation.

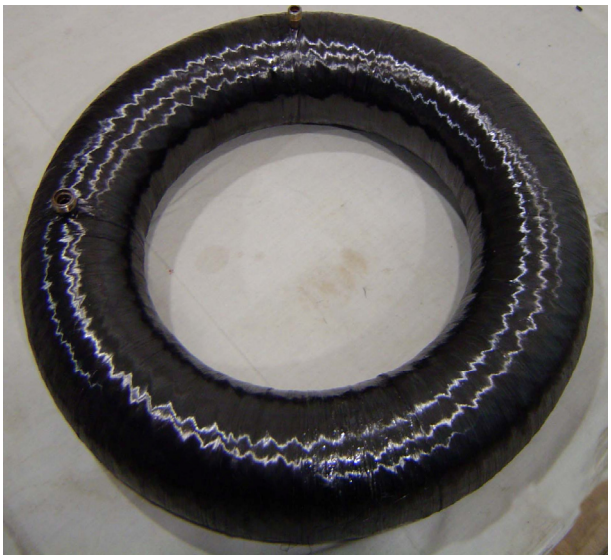

Fig.11. A finished toroidal pressure vessel wound by non-geodesic pattern

References

[1] Kim C. U., Kang J. H., Hong C. S. and Kim C. G. "Optimal design of filament wound structures under internal pressure based on the semi-geodesic path algorithm". *Compos. Struct.*, Vol. 67, No. 4, pp. 443-452, 2005.

[2] Koussios S, Bergsma O.K. and Beukers A. "Filament winding Part 1: Determination of the wound body related parameters". *Comp Part A: Appl Sci Manuf,* Vol. 35, No. 2, pp. 181-195, 2004.

[3] Koussios S, Bergsma O.K. and Beukers A. "Filament winding Part 2: Generic kinematic model and its solutions". *Comp Part A: Appl Sci Manuf,* Vol. 35, No. 2, pp. 197-212, 2004.

[4] Mazumdar S. K. and Hoa S. V. "Analytical models for low cost manufacturing of composite components by filament winding". *J. Compos. Mater.*, Vol. 29, No. 11, pp. 1515-1541, 1995.

[5] Fan L.Y. "Analysis of the Movement Law of the FRP Traffic Circle Pressure Vessel". *J. Wuhan Univ. of Tech.*, Vol. 22, No. 6, pp. 46-60, 2001.

[6] Li C.Y., Li F. A. and Zhang Q. "Fiber Path Analysis of Torus Pressure Vessel in Filament Winding". *Fiber Compos.*, No. 6, pp. 28-43, 2005.

[7] Wu M. H., Liang Y. D. and Yu Y. Y. "Stability of geodesic on torus", *Appl. Math.*, Vol. 16, No. 4, pp. 480-485, 2001.

[8] Zu L., He Q.X. and Li F.A. "Equicohesive winding linear design and stability analysis on toroidal pressure vessel". *J. Solid Rocket Tech.*, Vol. 29, No. 2, pp. 146-149, 2006.

[9] He, Q.X., Zu, L. and Li, F.A., "Design and optimization of winding parameters for filament-wound toroidal pressure vessels", *J. Astronautics*, Vol. 27, No. 6, pp. 240-245, 2006.

[10] Carvalho D. J., Lossie M., Vandepitte D. and Brussel V. H. "Optimization of Filament Wound Parts Based on Non-geodesic Winding". *Compos. Manuf.*, Vol. 6, No.2, pp.79-84, 1995.